

**ROLE OF THE STRUCTURE AND ELECTRONIC PROPERTIES OF  $\text{Fe}_2\text{O}_3$ – $\text{MoO}_3$  CATALYST ON THE DEHYDRATION OF ISOPROPYL ALCOHOL****Abd El-Aziz A. SAID***Department of Chemistry,  
Faculty of Science, Assiut University, Assiut, Egypt*

Received April 23, 1992

Accepted May 13, 1992

Molybdenum oxide catalysts doped or mixed with (1 – 50) mole %  $\text{Fe}^{3+}$  ions were prepared. The structure of the original samples and the samples calcined at 400 °C were characterized using DTA, X-ray diffraction and IR spectra. Measurements of the electrical conductivity of calcined samples with and without isopropyl alcohol revealed that the conductance increases on increasing the content of  $\text{Fe}^{3+}$  ions up to 50 mole %. The activation energies of charge carriers were determined in presence and absence of the alcohol. The catalytic dehydration of isopropyl alcohol was carried out at 250 °C using a flow system. The results obtained showed that the doped or mixed catalysts are active and selective towards propene formation. However, the catalyst containing 40 mole %  $\text{Fe}^{3+}$  ions exhibited the highest activity and selectivity. Correlations were attempted of the catalyst composition with their electronic and catalytic properties. Probable mechanism for the dehydration process is proposed in terms of surface active sites.

Molybdenum oxide catalysts, pure or mixed with foreign cations, play an important role in oxidation reactions<sup>1–7</sup>. It was observed that almost all good oxidation catalysts have sites associated with single valency changes of the cation. Such redox sites are often considered highly active both as adsorption sites and in electron exchange<sup>8,9</sup>.  $\text{Fe}_2\text{O}_3$ – $\text{MoO}_3$  catalysts are most widely used for the oxidation of methanol to formaldehyde. Extensive studies were concerned with the formation of iron molybdate spinel structure which shows a good activity and selectivity towards methanol oxidation to formaldehyde<sup>1–14</sup>. Bhattacharya et al.<sup>13</sup> reported that iron molybdate decomposes into  $\alpha$ - $\text{Fe}_2\text{O}_3$  and  $\text{MoO}_3$  on heating above 330 °C while Alessandrini et al.<sup>14</sup> suggested that the spinel is stable on heating up to 800 °C. However, the surface sites responsible for the reactions on the catalyst surfaces must be influenced by the change in the catalyst structure. Therefore, this work was devoted to characterization of the structure and active sites of the solid products of  $\text{Fe}_2\text{O}_3$ – $\text{MoO}_3$  system for doping as well as mixing. The structure was characterized by DTA, IR and X-ray diffraction. For the determination of active sites involved in the reaction, the catalytic decomposition of isopropyl alcohol together with the electrical conductivity in situ has been used as relevant methods.

## EXPERIMENTAL

### Materials

Reagent grade chemicals were used in this work. A known weight of ammonium molybdate,  $(\text{NH}_4)_6\text{Mo}_7\text{O}_{24} \cdot 4 \text{H}_2\text{O}$ , was impregnated with the appropriate amount of  $\text{Fe}(\text{NO}_3)_3 \cdot 9 \text{H}_2\text{O}$  solutions with vigorous stirring at room temperature. The impregnated solids were dried at 100 °C in an oven to constant weight and calcined in air at 400 °C for 4 h. The content of  $\text{Fe}^{3+}$  ions added varied between 1 to 50 mole %.

### Apparatus and Techniques

Differential thermal analysis (DTA) of pure ammonium molybdate (AM) and the molybdate mixed with  $\text{Fe}^{3+}$  ions was carried out using a Shimadzu Computerized Thermal Analysis System DT-40. The system includes programmes which process data from the thermal analyzer with the chromatopac C-R3A. The rate of heating was kept at 10 °C min<sup>-1</sup> in presence of air flow (40 ml min<sup>-1</sup>).  $\alpha$ -Alumina powder for DTA standard material was applied as a reference.

Infrared spectra of the solid products were recorded using Perkin-Elmer Model SP3-300 infrared spectrophotometer in the range 1 200 – 200 cm<sup>-1</sup>, using KBr disc technique. X-Ray diffraction patterns were recorded on a Philips diffractometer (model PW 1010). The patterns were obtained with Ni filter and Cu radiation. The diffraction lines were matched with ASTM cards<sup>15</sup>. The electrical conductivity measurements were carried out using a conductivity cell described previously<sup>16</sup>.

The catalytic activity was tested using the vapour-phase decomposition of isopropyl alcohol (IPA) in a conventional gas flow system at atmospheric pressure. The system consisted of two reactors; one of them was used without any catalyst (control reactor), which enabled measurement of the blank conversion which was subtracted from that measured with the flow reactor. A reaction gas mixture of IPA with air was introduced into the fixed bed flow reactor. The exit feed was analyzed by direct sampling of the gaseous products into a PYE Unicam gas chromatograph equipped with a column of 3 m length and 0.5 cm diameter filled with 20% PEG and maintained at 100 °C.

## RESULTS AND DISCUSSION

### *Differential Thermal Analysis*

Figure 1 represents DTA curves of pure AM and the ammonium molybdate mixed with 30, 40 and 50 mole % of  $\text{Fe}^{3+}$  ions. Curve *a* of pure AM exhibits four endothermic peaks. The first peak with maximum at 124 °C indicates removal of four water crystallization molecules bound to AM molecules<sup>17</sup>. The second one located at 204 °C corresponds to the formation of the intermediate  $(\text{NH}_4)_2\text{O}_4\text{MoO}_3$ , whereas the third peak at 300 °C is due to the decomposition of this intermediate into  $\text{MoO}_3$  (ref.<sup>18</sup>). The fourth peak at 780 °C can be attributed to the sublimation of  $\text{MoO}_3$  solid<sup>19</sup>. The addition of 30 mole %  $\text{Fe}^{3+}$  ions (curve *b*) shows that the decomposition proceeds in three decomposition stages. The first endothermic peak located at 235 °C is probably due to the loss of water of crystallization of the iron molybdate formed at this stage together with the formation of the intermediate  $(\text{NH}_4)_2\text{O}_4\text{MoO}_3$ . The second endothermic peak at 294 °C corresponds to the decomposition of the intermediate yielding in the first stage into  $\text{MoO}_3$ . The third endothermic peak with maximum at 776 °C is attributed to

the sublimation of  $\text{MoO}_3$ . In fact, the decrease in the peak area corresponding to the decomposition of the intermediate indicates the participation of AM in the formation of iron molybdate. On increasing the ratios of  $\text{Fe}^{3+}$  ions, (curves *c* and *d*), the thermal decomposition proceeds in one stage on heating up to 800 °C. The endothermic peak at 235 °C corresponds to the loss of water molecules, indicating that iron molybdate catalyst gets completely dehydrated above this temperature<sup>13</sup>. Moreover, the absence of any peaks on heating up to 800 °C indicates the higher stability of the solid product and no excess  $\text{MoO}_3$  included. Bhattacharya et al.<sup>13</sup> concluded that above 330 °C iron molybdate starts to decompose to amorphous ferric oxide and molybdenum oxide. It is clear from the above results that iron molybdate spinel is stable on heating up to 800 °C, which is good agreement with the results obtained by Alessandrini et al.<sup>14</sup>. Finally, two endothermic peaks at 126 and 166 °C, respectively, may be attributed to the decomposition of ammonium nitrate formed in the reaction mixture<sup>20</sup>.

### X-Ray Diffraction

Figure 2 shows the XRD patterns of pure  $\text{MoO}_3$  and that mixed with 20, 30, 40 and 50 mole %  $\text{Fe}^{3+}$  ions preheated in air at 400 °C for 4 h. Curves *b* and *c* show characteristic

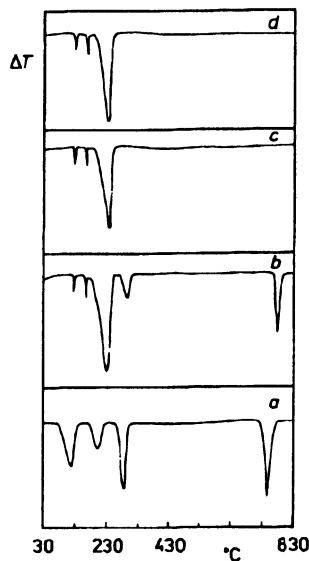


FIG. 1  
DTA curves of pure AM (*a*) and mixed with  $\text{Fe}^{3+}$  ions: 30 mole % (*b*), 40 mole % (*c*) and 50 mole % (*d*)

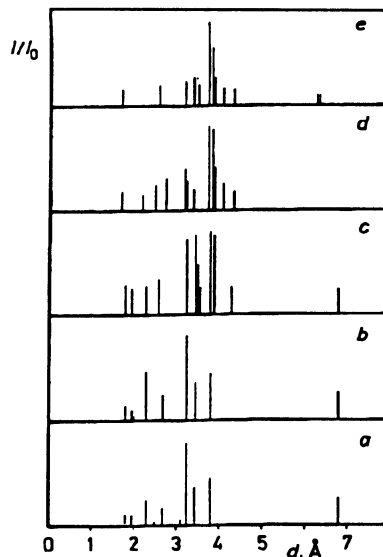


FIG. 2  
X-Ray diffraction of pure  $\text{MoO}_3$  (*a*) and  $\text{MoO}_3$  mixed with  $\text{Fe}^{3+}$  ions: 20 mole % (*b*), 30 mole % (*c*), 40 mole % (*d*) and 50 mole % (*e*). The samples were calcined at 400 °C for 4 h

lines of  $\text{MoO}_3$  and the iron molybdate  $\text{Fe}_2(\text{MoO}_4)_3$ . The presence of  $\text{MoO}_3$  can be deduced from the occurrence of the lines at  $d(\text{\AA}) = 3.81, 3.49, 3.25$ , whereas the characteristic lines corresponding to the  $\text{Fe}_2(\text{MoO}_4)_3$  phase<sup>14</sup> are located at  $d(\text{\AA}) = 4.07, 3.86, 3.46$  and  $2.96$ . Curves **d** and **e** correspond to the  $\text{MoO}_3$  mixed with 40 or 50 mole %  $\text{Fe}^{3+}$  ions, indicating that the characteristic lines of  $\text{MoO}_3$  could not be detected. However, the detected lines confirm the formation of iron molybdate. These results demonstrate that the iron molybdate spinel can be formed without excess  $\text{MoO}_3$  in the presence of 40 mole %  $\text{Fe}^{3+}$  ions.

### IR Spectra

IR spectra of  $\text{Fe}_2\text{O}_3$ – $\text{MoO}_3$  catalysts calcined at 400 °C are shown in Fig. 3. Curve 1 shows the absorption bands at 990 and 870  $\text{cm}^{-1}$  assigned to the double bonded oxygen  $\text{Mo}=\text{O}$  and to Mo–O–Mo lattice vibration modes<sup>21,22</sup>. Curve 2 shows that the addition of 30 mole %  $\text{Fe}^{3+}$  ions leads to a little lattice distortion of  $\text{MoO}_3$ . On addition of 40 or 50 mole %  $\text{Fe}^{3+}$  ions (curves 3 and 4) the absorption bands corresponding to  $\text{MoO}_3$  are absent and new bands at 930, 420 and 340  $\text{cm}^{-1}$  can be attributed to the formation of iron molybdate<sup>23</sup>. The results of interest are in Fig. 4 for IR spectra of the original

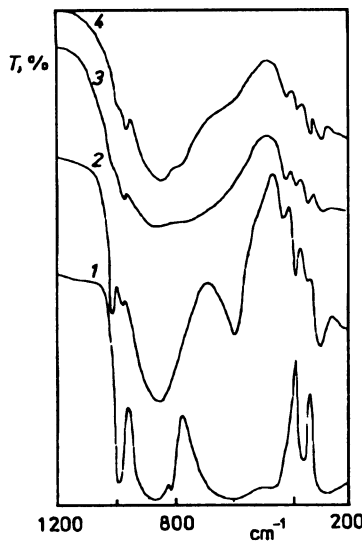


FIG. 3  
IR Spectra of pure  $\text{MoO}_3$  (1) and  $\text{MoO}_3$  mixed with  $\text{Fe}^{3+}$  ions: 30 mole % (2), 40 mole % (3) and 50 mole % (4). The samples were calcined at 400 °C for 4 h

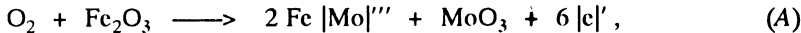


FIG. 4  
IR Spectra of the AM mixed with  $\text{Fe}^{3+}$  ions: 30 mole % (1), 40 mole % (2) and 50 mole % (3)

samples of  $\text{MoO}_3$  mixed with 30, 40 or 50 mole %  $\text{Fe}^{3+}$  ions. It appears that the bands correspond to the iron molybdate located at the same position as that of the samples calcined at 400 °C.

### Electrical Conductivity

Electrical conductivity measurements with and without IPA vapour atmosphere have been carried out at 250 °C on all the catalysts calcined at 400 °C. The experimental conditions used were 0.5 g catalyst and 1.7% reactant of IPA vapour in the gas feed. The flow rate of the carrier gas was 300 ml min<sup>-1</sup> (STP). The equilibrium conditions were obtained within 20 – 60 min, depending on the catalyst composition and the reaction temperature. Figure 5 shows the variation of  $\log \sigma$  with the catalyst composition. Curve 1 shows that without IPA (air only), the conductance increases on increasing content of  $\text{Fe}^{3+}$  ions up to 50 mole %. This behaviour indicates that the presence of  $\text{Fe}_2\text{O}_3$  increases the charge carriers within  $\text{MoO}_3$  lattice. This can be attributed to the creation of holes via  $\text{Mo}^{6+}$  substituted  $\text{Fe}^{3+}$  (Eq. (A))



where  $\text{Fe} |\text{Mo}|'''$  is a  $\text{Fe}^{3+}$  cation substituting a lattice  $\text{Mo}^{6+}$  and  $|\text{e}|'$  is a hole. The creation of holes should enhance the electron mobility within  $\text{MoO}_3$  lattice and consequently, it increases its conductance. The effects of (IPA–air) mixture on the conductance values are shown in Fig. 5 (curve 2). It appears that the conductance is higher than that obtained in presence of air only. This indicates the increase of the charge carriers on the catalyst surface via the electron injected by IPA to the available accepting sites. The electronic theory of chemisorption on semiconducting materials postulates<sup>24</sup> a close relation between the electronic properties of a catalyst and its catalytic activity. The width of the energy gap is important in controlling the number of molecules which can be chemisorbed in the course of a catalytic reaction and the nature

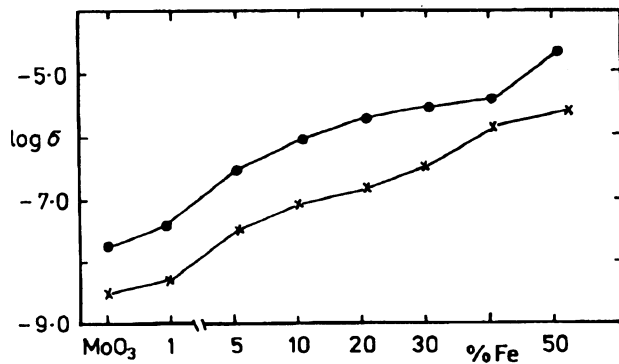


FIG. 5  
The variation of  $\log \sigma$  with the percentual concentration of  $\text{Fe}^{3+}$  ions (mol/mol) without IPA (1) and with IPA (2)

of the chemical bond between the molecule and the surface. These factors control at the same time the catalyst activity and the mechanism of the catalytic reaction. Accordingly, the influence of the reaction temperature on the conductance with and without IPA was studied in the range 150 – 300 °C. The results indicated that the electronic exchange, i.e. the conductance value, increases on increasing the reaction temperature. Plots of  $\log \sigma$  against  $1/T$  of pure  $\text{MoO}_3$  and mixed with  $\text{Fe}^{3+}$  ions can be fitted to an Arrhenius relationship<sup>25</sup>

$$\sigma = \sigma_0 \exp^{-E_a/RT}, \quad (1)$$

where  $E_a$  is the activation energy for conduction. Values of  $E_a$  obtained by the least squares fitting of data are given in Table I.

Such results show that the doped and mixed catalysts are active and selective towards propene formation, compared to the pure  $\text{MoO}_3$  catalyst. Moreover, the catalyst with 40 mole %  $\text{Fe}^{3+}$  ions exerts the highest activity and selectivity for the dehydration process. Furthermore, the dehydrogenation process is little affected by varying the catalyst composition. This means that the addition of  $\text{Fe}_2\text{O}_3$  only improves the sites responsible for the dehydration reaction. Therefore, only dehydration reaction is dealt with in the following discussion.

From Table I, it can be easily seen that in the absence of IPA the activation energies decrease on increasing  $\text{Mo}^{6+}$  substitution with  $\text{Fe}^{3+}$  ions. The decrease in  $E_a$  values may be ascribed to the start of the formation of iron molybdate spinel structure and it is consistent with the pairing probability for the charge transfer proposed for the hopping model. It was suggested<sup>25 – 27</sup> that the charge carrier moves through the hopping polarons, which consists of a  $d$ -electron and its polarized region in the lattice. In the observed minimum for the composition containing 40 mole %  $\text{Fe}^{3+}$  ions, the optimum Fermi potential may be established<sup>28</sup>. A further decrease in the activation energies in the presence of (IPA + air) is obtained. This behaviour is probably due to the pinning of the Fermi energy to stabilize the density of electrons in the conduction band<sup>28</sup>.

TABLE I  
The electronic exchange  $E_a$  (in eV) for pure  $\text{MoO}_3$  and  $\text{MoO}_3$  mixed with  $\text{Fe}^{3+}$  ions

Catalyst	$E_a$ (air)	$E_a$ (air + IPA)
Pure $\text{MoO}_3$	0.92	0.81
+ 20 mole % $\text{Fe}^{3+}$	0.84	0.71
+ 30 mole % $\text{Fe}^{3+}$	0.65	0.53
+ 40 mole % $\text{Fe}^{3+}$	0.41	0.38
+ 50 mole % $\text{Fe}^{3+}$	0.66	0.56

### Catalytic Activity Measurements

The catalytic activity of various solids for isopropyl alcohol dehydration was determined using the same conditions as used for the electrical conductivity. The reaction products were propene with a minor yield of acetone. No products other than propene and acetone were detected. The experimental results are presented in Table II.

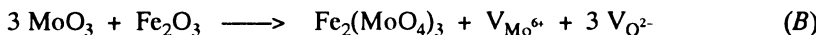
Based on the electron-donating nature<sup>29</sup> of the dehydration reaction of IPA, one can explain the higher activity and selectivity of  $\text{FeO}_3\text{-MoO}_3$  catalysts in terms of the coordination and electronic state of the active sites exposed in the surface planes, which in turn is influenced by the electron availability at the surface. Although each plane is electrically neutral overall, many surface sites may not all be neutral but may have local positive or negative charges, and the lowered coordinations. These sites well seek to be neutralized by electron movement, either by adsorption of an electron donor molecule, or by electron movement from the bulk of the solid<sup>30</sup>. Accordingly, as based on the available data, the increase in the dehydration reaction on addition of  $\text{Fe}_2\text{O}_3$  up to 10 mole % may be explained on the basis of the doping effect of  $\text{Fe}^{3+}$  ions, according to Eq. (A). The creation of holes together with  $\text{Mo}^{6+}$  should enhance the chemisorption of IPA and consequently should increase the dehydration reaction<sup>31,32</sup>. This suggestion accords with the increase in  $\log \sigma$  values (Fig. 5). The highest activity and selectivity of  $\text{Fe}_2(\text{MoO}_4)_3$  spinel can be explained on the basis of its structure favouring adsorption and activation of IPA. It was reported that<sup>33</sup> the formation of iron molybdate is accompanied with the generation of molybdenum vacancies  $\text{V}_{\text{Mo}}^{6+}$  and oxygen vacancies  $\text{V}_{\text{O}^{2-}}$  (Eq. (B)).

TABLE II

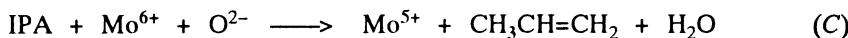
Dehydration of isopropyl alcohol (conversion, yield and selectivity in %) on pure  $\text{MoO}_3$  and on  $\text{MoO}_3$  mixed with  $\text{Fe}^{3+}$  ions at 250 °C

% $\text{Fe}^{3+}$ <sup>a</sup>	Conversion %	Yield (in %) of		Selectivity (in %) to	
		propene	acetone	propene	acetone
$\text{MoO}_3$	80.6	73.5	5.0	91.2	6.2
1	85.5	78.5	3.8	91.8	4.4
5	89.5	82.3	2.5	92.0	2.8
10	91.2	85.1	1.5	93.3	1.6
20	92.5	87.5	1.4	94.6	1.5
30	94.1	89.5	1.4	95.1	1.5
40	98.5	97.0	1.4	98.5	1.4
50	88.5	82.0	2.6	92.6	2.9

<sup>a</sup> mol/mol  $\text{MoO}_3$ .



Moreover, it was suggested<sup>20</sup> that the large density oxygen vacancies in the active catalyst could be the partially occupied donors. These provide an impurity band that acts as a source and sink of electrons. From the activation energies, it can be concluded that the decrease in its values should be facilitated by the electron exchange between IPA and the accepting sites on the catalyst surface during the reaction. In addition, Trifiro et al.<sup>34</sup> concluded that the whole catalyst (iron molybdate) participates in the reaction of methanol. This supports the idea that iron cations participate in the reaction pathways. Accordingly, based on the model proposed by earlier workers<sup>35,36</sup>, the dehydration of IPA can occur on a pair of adjacent sites ( $\text{Mo}^{6+}$  and  $\text{O}^{2-}$  as acidic and basic sites, respectively). However, the dehydration reaction of IPA can proceed as follows.



It was reported<sup>37</sup> that the role of iron is to transfer water and oxygen between the catalyst surface and the gas phase. According to the above mechanism and based on the obtained results, it is clear that  $\text{Fe}^{3+}$  ions hinder the reduction of  $\text{Mo}^{6+}$  cation, which is consistent with the results reported<sup>38,39</sup>. Thus, the presence of  $\text{Mo}^{6+}/\text{Mo}^{5+}$  and  $\text{Fe}^{3+}/\text{Fe}^{2+}$  as a redox cycles together with  $\text{O}^{2-}$  represents the active and selective surface sites. On the other hand, the decrease in the activation energies during the reaction of IPA may be attributed to the hopping mechanism of these cycles.

## REFERENCES

1. El-Awad A. M., Hassan E. A., Said A. A., Abd El-Salaam K. M.: Monatsh. Chem. 120, 199 (1989).
2. Haber J., Mielczewska E., Turek W.: Z. Phys. Chem. 144, 69 (1985).
3. Goldets G. I.: *Studies in Surface Science and Catalysis*, Vol. 15, *Heterogeneous Catalytic Reduction Involving Molecular Oxygen*, Chap. XVI. Elsevier, Amsterdam 1983.
4. Machiels C. J.: ACS Symp. Ser. 178, 239 (1982).
5. Allison J. N., Godard W. A.: J. Catal. 92, 127 (1985).
6. Arnoldy P., Franken M. C., Sheffer P., Moulijn J. A.: J. Catal. 96, 38 (1985).
7. Satsumu A., Hattori A., Mitzutani K., Furuta A., Miyamoto A., Hittori T., Murikami Y.: J. Phys. Chem. 93, 1484 (1989).
8. Peacock J. M., Parker A. J., Ashimore P. G., Hockey J. A.: J. Catal. 15, 373 (1969).

9. Schuit G. C. A.: *J. Less-Common Met.* **36**, 329 (1974).
10. Carbucicchio M., Trifiro F.: *J. Catal.* **45**, 77 (1976).
11. Machiels C. J., Sleight A. W.: *J. Catal.* **76**, 238 (1982).
12. Machiels C. J., Sleight A. W.: *Proceedings of the 4th Int. Conf. on Chemistry and Uses of Molybdenum, Golden, Colorado 1982*, p. 411.
13. Bhattacharya P. K., De P. P., Jayannathan R., Bhattacharya S. K.: *Ind. Chem.* **14**, 973 (1976).
14. Alessandrini G., Cairati L., Forzatti P., Villa P. L., Trifiro F.: *J. Less-Common Met.* **54**, 373 (1977).
15. McClune W. F. (Ed.): *Powder Diffraction File (Inorganic Compounds)*, JCPDS, PA 1978.
16. Abd-El-Salaam K. M., Said A. A.: *Surf. Technol.* **17**, 199 (1982).
17. Ibrahim A. A., El-Shobaky G. A.: *Thermochim. Acta* **147**, 175 (1989).
18. Yong W. J.: *Thermochim. Acta* **158**, 183 (1990).
19. *Handbook of Chemistry and Physics*, p. 610. The Chemical Rubber Publishing Company, Cleveland 1961.
20. Notz K. J., Hass P. A.: *Thermochim. Acta* **155**, 283 (1989).
21. a) Trifiro F., Pasquon I.: *J. Catal.* **12**, 412 (1968); b) Mitchell P. C. H., Trifiro F.: *J. Chem. Soc., A* **1970**, 3183.
22. Ferraro J. R.: *Low Frequency Vibration of Inorganic and Coordination Compounds*. Plenum Press, New York 1971.
23. Villa P. L., Szabo A., Trifiro F., Carbucicchio M.: *J. Catal.* **47**, 122 (1977).
24. Hauffe K.: *Adv. Catal.* **7**, 213 (1955).
25. Dissanayake M. A., Illeperuma O. A., Dharmasena P. A.: *J. Phys. Chem. Solids* **50**, 352 (1989).
26. Pomonis P., Vickerman J. C.: *J. Catal.* **55**, 88 (1978).
27. Kumar D., Parsad C. D., Parkash O.: *J. Phys. Chem. Solids* **51**, 73 (1990).
28. Kimoto K., Mirroson S. R.: *Z. Phys. Chem.* **108**, 11 (1977).
29. Said A. A., Hassan E. A., El-Awad E. M., Abd El-Salaam K. M.: *Collect. Czech. Chem. Commun.* **54**, 1508 (1989).
30. Odumah E. I., Vickerman J. C.: *J. Catal.* **62**, 195 (1980).
31. Giordana N., Measa M., Costellan A., Bart J. C. J., Ragaini V.: *J. Catal.* **50**, 342 (1977).
32. Vaishnava P. P., Monatano P. A., Tisher R. E., Pollack S. S.: *J. Catal.* **78**, 454 (1984).
33. Halawy S. A.: *Ph.D. Thesis*. Assiut University, Assiut 1989.
34. Trifiro F., Notarbartoloo S., Pasquon I.: *J. Catal.* **22**, 324 (1971).
35. Hussein G. A. M., Sheppard N., Zakai M. I., Fahim R. B.: *J. Chem. Soc., Faraday Trans. 1* **85**, 1723 (1989).
36. Said A. A.: *Collect. Czech. Chem. Commun.* **50**, 2807 (1991).
37. Trifiro F., DeVecchi V., Pasquon I.: *J. Catal.* **15**, 8 (1969).
38. Pernicone N., Lazzerin F., Liberti G., Lanzavecchia G.: *J. Catal.* **14**, 293, 391 (1969).
39. Nováková J., Jírů P., Zavadil V.: *J. Catal.* **21**, 143 (1971).

Translation revised by J. Hetflejš.